Drug Design, Development and Therapy

Dovepress
open access to scientific and medical research

Open Access Full Text Article

ORIGINAL RESEARCH

Silibinin Schiff Base Derivatives Counteract CCl_4-Induced Acute Liver Injury by Enhancing Anti-Inflammatory and Antiapoptotic Bioactivities

Rong Xu[1,*], Siyan Qiu[1,*], Jie Zhang[1], Xiaoli Liu[1], Ling Zhang[1], Haizhu Xing[1], Min You[1], Man Wang[1], Yuting Lu[1], Peng Zhang[1], Jing Zhu[1,2]

[1]Jiangsu Key Laboratory for Pharmacology and Safety Evaluation of Chinese Materia Medica, School of Pharmacy, Nanjing University of Chinese Medicine, Nanjing, People's Republic of China; [2]Department of Neurology and Neuroscience, Johns Hopkins School of Medicine, Baltimore, MD, USA

*These authors contributed equally to this work

Correspondence: Jing Zhu, Jiangsu Key Laboratory for Pharmacology and Safety Evaluation of Chinese Materia Medica, Department of Pharmacy, Nanjing University of Chinese Medicine, Nanjing, 210023, People's Republic of China, Tel +86-15895975410, Email 830640@njucm.edu.cn

Background: Silibinin (Sil), a flavonoid lignan-like natural compound derived from milk thistle seeds, has been used to treat hepatic diseases, including early-phase hepatocirrhosis and fatty liver, for many years. However, its poor water solubility limits its gastrointestinal absorption and bioavailability. It clinical use has been limited due to its slow onset of action. Faced with this problem, research on the derivatives of silibinin has been receiving much attention.

Purpose: A series of silibinin derivatives with good biosafety and higher hepatoprotective activity were obtained by a safe, efficient and green chemical synthesis method.

Patients and Methods: First, the carbonyl group in the structure of silibinin was used to obtain silibinin Schiff base derivatives by dehydration condensation with the carboxyl group in the sulfur-containing amino acid. Next, relevant experiments were performed to characterize the structure, physical form and solubility of the derivatives. Then, toxicity tests of the derivatives were performed in LO-2 cells and SD rats to evaluate their biosafety. Finally, the anti-inflammatory and antiapoptotic activities were observed using a carbon tetrachloride (CCl_4)-induced acute liver injury model in C57BL/6J mice using silibinin as a control.

Results: The studies showed that SS and ST behaved as amorphous substances and showed a significant increase in solubility compared to silibinin. These two derivatives showed low toxicity in biosafety tests and higher bioactivity (anti-inflammatory and anti-apoptotic) than silibinin against acute liver injury induced by CCl_4.

Conclusion: Two silibinin derivatives (SS and ST) obtained by the Schiff base reaction improved the solubility of the silibinin parent nucleus in biological media with the help of the hydrophilic and amorphous morphology of the ligand. The low toxicity in vivo and in vitro ensures the biosafety of the derivatives. The hepatoprotective activity (anti-inflammatory and anti-apoptotic) was significantly improved compared to silibinin.

Keywords: silibinin, sulfur-containing amino acid, Schiff base, solubility, inflammation, apoptosis

Introduction

Silibinin (Sil), a representative constituent extracted from silibinin seeds,[1] exhibits a variety of activities in terms of therapeutic characteristics, including antioxidant, anti-inflammatory, anticancer, and antiviral activities. In particular, its powerful and rich hepatoprotective effects have been confirmed in both basic research and clinical practice.[2–5] However, the extremely low water solubility of silibinin results in its poor bioavailability.[6,7] As a result, the pharmacological activity of silibinin is affected.

Received: 2 January 2022
Accepted: 5 May 2022
Published: 16 May 2022

To overcome this drawback of silibinin, many semisynthetic derivatives and preparations have been developed via chemical structure modification.[8] Rich derivatives, such as glycosides, esters, and ethers, are obtained mainly by attacking the five hydroxyl groups in the structure of silibinin. The compounds that have been widely used in the clinic are bis-hemisuccinate and methylglucamine salt,[9–11] and these have shown greatly improved water solubility. However, in the present study, molecular docking simulations of silibinin with certain proteins at the initial stage revealed that their binding relies mainly on the hydroxyl groups in its structure and amino acids in the protein structure (Figure S1). Although these proteins are not necessarily the targets of silibinin, there are still implications for how molecules and proteins interact. Therefore, disruption of the mid-hydroxyl site of the silibinin structure may affect its pharmacological activity. Many delivery strategies can improve the absorption and bioavailability of silibinin from a formulation perspective, such as nanoparticles, polymeric particles, and phospholipid complexes.[6,12–17] Nevertheless, much work remains for the industrial production of most of the formulations due to their low drug loading capacity, storage difficulties, complicated process, and poor reproducibility.

Therefore, we selected the carbonyl side of silibinin for the Schiff base reaction and selected several sulfur-containing amino acids as hydrophilic ligands. On the one hand, the solubility of silibinin is improved by the hydrophilic nature of the ligand; on the other hand, the hepatoprotective activity of silibinin can be further improved with the help of the biological properties of singlet sulfur in redox reactions.[18–22]

In this study, acute liver injury caused by carbon tetrachloride (CCl_4) was selected as an animal model to evaluate the biological activity of the two Schiff base derivatives. CCl_4-induced liver injury has been widely used as a classical model of acute liver injury to measure the hepatoprotective activity of drugs;[23–26] additionally, the pathological mechanisms of inflammation and apoptosis induced by CCl_4 in the liver can better simulate acute chemical liver injury in humans. In response to these two aspects of disease pathogenesis, silibinin has shown some therapeutic effects in the study of a variety of conditions.[5,27,28]

In summary, this study aimed to obtain several silibinin Schiff base derivatives by condensation of silibinin with certain sulfur-containing hydrophilic ligands through a Schiff base reaction. Chemical structure characterization, physicochemical property analysis, in vitro and in vivo biosafety evaluation and in vivo bioactivity (hepatoprotective activity)-related experiments were also performed to evaluate the safety and efficacy of these silibinin derivatives.

Materials and Methods

Materials

Silibinin (purity: 98%), S-Allyl-L-cysteine (purity: ≥98%), and taurine (purity: 99%) were supplied by Shanghai Aladdin Biochemical Technology Co. All other purchased solvents are of analytical grade.

The Synthesis Method of SS and ST

NaOH (1 mmol) and an equal stoichiometric quantity of S-allyl-L-cysteine or taurine (1 mmol) were placed in a three-necked flask preloaded with a magnetic stirrer, and 5 mL of water was then added dropwise and stirred until the solid compound was completely dissolved to obtain Solution A. Silibinin (1 mmol) was dissolved in 45 mL of anhydrous ethanol by heating in a water bath to obtain solution B. Solution A was added dropwise into solution B, while anhydrous sodium sulfate was added for dehydration and stirred for 2 h at 60 °C. After the reaction was completed, the hot mixed solution was extracted, and the filtrate was rotary evaporated to obtain the crude product. Finally, the crude product was recrystallized by anhydrous ethanol and dried under a vacuum to obtain the corresponding pure product (SS (Figure 1A) or ST (Figure 1B)).

SS: Yield 72%, the bright yellow powder solid. 1H NMR (500 MHz, DMSO) δ 7.03 (dd, J = 3.4, 1.8 Hz, 1H), 7.01 (s, 1H), 6.99–6.97 (m, 1H), 6.95 (dd, J = 8.3, 1.8 Hz, 1H), 6.86 (d, J = 8.2 Hz, 1H), 6.82 (d, J = 8.1 Hz, 1H), 5.77 (ddt, J = 17.0, 10.0, 7.1 Hz, 1H), 5.45–5.37 (m, 2H), 5.14 (d, J = 17.0 Hz, 1H), 5.06 (d, J = 10.0 Hz, 1H), 4.90 (dd, J = 7.9, 1.5 Hz, 1H), 4.86 (d, J = 10.7 Hz, 1H), 4.35 (dd, J = 10.7, 8.1 Hz, 1H), 4.18–4.13 (m, 1H), 3.78 (s, 3H), 3.54 (dd, J = 12.1, 2.1 Hz, 1H), 3.45 (q, J = 7.0 Hz, 2H), 3.34 (dd, J = 12.2, 4.6 Hz, 1H), 3.21–3.11 (m, 3H), 2.88 (dd, J = 13.5, 3.7 Hz, 1H), 2.58–2.52 (m, 1H) (Figure S2A). 13C NMR (126 MHz, DMSO) δ 173.21, 164.03, 162.23, 148.12, 147.63, 143.70, 135.20, 131.50, 127.83, 121.54, 120.96, 117.40, 116.87, 116.63, 115.78, 112.12, 98.76, 98.13, 97.11, 82.40, 78.59, 76.33, 71.65, 60.65, 56.48, 56.13, 55.04, 34.36, 19.03 (Figure S2B).

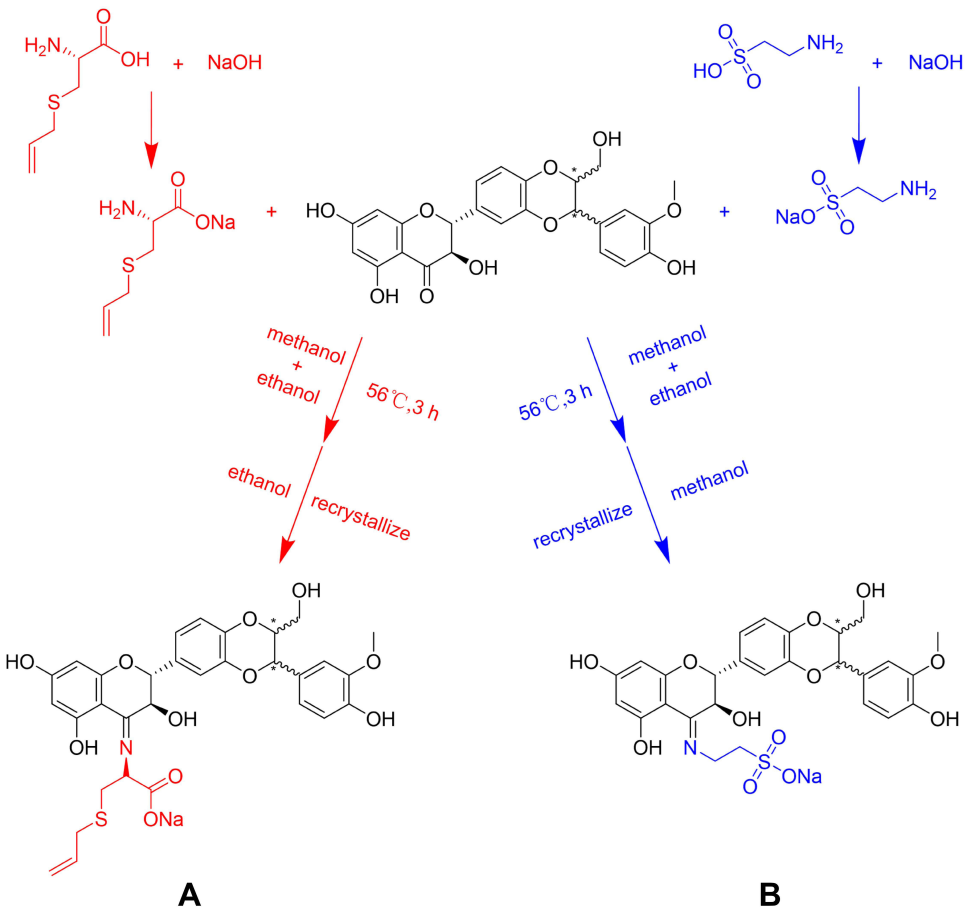

Figure 1 Synthesis method of compounds. The chemical structures of SS (**A**) and ST (**B**).

ST: Yield 74%, the dark red powder solid. 1H NMR (500 MHz, DMSO) δ 7.05 (dd, J = 3.5, 1.9 Hz, 1H), 7.01 (s, 1H), 7.00–6.97 (m, 1H), 6.95 (d, J = 1.7 Hz, 1H), 6.86 (d, J = 8.2 Hz, 1H), 6.81 (d, J = 8.1 Hz, 1H), 5.55–5.47 (m, 2H), 4.92 (d, J = 3.5 Hz, 1H), 4.90 (s, 1H), 4.41 (dd, J = 10.8, 8.0 Hz, 1H), 4.19–4.12 (m, 1H), 3.78 (s, 3H), 3.54 (dd, J = 12.2, 2.2 Hz, 1H), 3.45 (q, J = 7.0 Hz, 2H), 3.34 (dd, J = 12.2, 4.6 Hz, 1H), 2.89 (t, J = 6.4 Hz, 2H), 2.60 (t, J = 6.4 Hz, 2H) (Figure S2C). 13C NMR (126 MHz, DMSO) δ 164.01, 162.43, 148.10, 147.56, 143.87, 143.62, 131.33, 127.89, 120.97, 116.99, 116.71, 115.76, 112.15, 98.28, 97.90, 97.54, 82.56, 78.56, 76.32, 71.66, 60.65, 56.48, 56.14, 52.12, 37.88, 19.03 (Figure S2D).

Powder X-Ray Diffraction (PXRD)

PXRD analysis was performed on a LYNXEYE_XE_T (1D mode) diffractometer pattern using Cu/K-Alpha1 (λ=1.5406 Å) radiation at room temperature. The instrument was operated at 40 kV and 40 mA. Data acquisition was performed from 3° to 40° (2θ) with a step size of 0.02°. Before sending the sample for testing, approximately 5 mg of the powder was weighed and gently pressed with a silicon wafer to obtain a flat powder bed surface.

In vitro Solubility Test

A certain mass of SS and ST was accurately weighed into an 8 mL glass vial. Five milliliters of various standard buffer solutions were added separately. The preparation methods of the six standard buffer solutions are shown in Table 1. The obtained solutions were stirred at 37 °C at 400 rpm and sampled at 0.25 hours, 0.5 hours, 1 hour, 2 hours, and 24 hours. The samples were centrifuged at 37 °C at 14,000 rpm for 5 min. Supernatants were analyzed by HPLC and pH meter for solubility and pH value, respectively.

Table 1 Configuration of Six Standard Buffers

No.	ID	pH	Composition
ES1	HCl solution	1.0	Pipetted 4.55 mL of hydrochloric acid (37% HCl) into 500 mL deionized water. Mixed well.
ES2	Acetate buffer	4.5	Placed 1.495 g sodium acetate trihydrate in a 500 mL volumetric flask, added 7 mL 2 N acetic acid, then added deionized water to volume, and mixed well.
ES3	Phosphate buffer	6.8	Placed 125 mL of the monobasic potassium phosphate solution in a 500 mL volumetric flask, added 56 mL of the 2 N sodium hydroxide solution, then added deionized water to volume.
ES4	SGF	2.0	Step 1: Weighed 2 g of sodium chloride (NaCl) and 1 g of Triton X-100 into a 1000 mL flask followed by the addition of approximately 800 mL of deionized water. The mixture was stirred until all solids were dissolved. Added approximately 100 mL of 0.1 N HCl, checked pH value with a pH meter, and adjusted the pH to 2.0 with HCl (1 N) or NaOH (1 N). Then, diluted to the volume with deionized water.
ES5	FaSSIF	6.5	Step 1: Placed 0.210 g sodium hydroxide, 2.235 g sodium dihydrogen phosphate, and 3.093 g sodium chloride in a 500 mL volumetric flask; added approximately 0.450 L deionized water; and adjusted the pH to 6.5 with 1N sodium hydroxide or 1 N hydrochloric acid. Made up to volume (0.5 L) with deionized water. Step 2: Placed and dissolved 1.120 g FaSSIF/FeSSIF/FaSSGF instant powder in 0.250 L of buffer (from step 1) in a 500 mL volumetric flask and then added buffer (from step 1) to volume and mixed well.
ES6	FeSSIF	5.0	Step 1: Placed 2.020 g sodium hydroxide, 4.325 g acetic acid, and 5.937 g sodium chloride in a 500 mL volumetric flask; added approximately 0.450 L deionized water; and adjusted the pH to 5.0 with 1 N sodium hydroxide or 1 N hydrochloric acid. Made up to volume (500 mL) with deionized water. Step 2: Placed and dissolved 5.600 g FaSSIF/FeSSIF/FaSSGF instant powder in 0.250 L of buffer (from step 1) in a 500 mL volumetric flask and then added buffer (from step 1) to volume and mixed well.

Cytotoxicity Assay

The human normal liver cell line LO-2 (HL-7702) was purchased from the Cell Bank of Chinese Academy of Sciences (Shanghai, China). LO-2 cells were maintained in DMEM (HyClone, #SH30243.01, Logan) with 10% fetal bovine serum (Gibco, #16140071, New York) in a humidified 5% CO_2 incubator at 37 °C. According to the cell size and growth rate, 1×10^4 cells per well were inoculated into a 96-well cell culture well plate, and the subsequent procedure was performed when the cell density reached 70–80%. Different concentrations of drugs were added for stimulation, and appropriate controls were set up. Detailed subsequent steps can be found in the LDH Cytotoxicity Assay Kit (Beyotime, #C0016, Shanghai)[29,30] and Cell Counting Kit-8 (Yeasen, #40203ES60, Shanghai)[31,32] instructions.

Acute Oral Toxicity

Male SD rats (8–10 weeks, 190–210 g) were purchased from Weitonglihua (Nanjing, China) and housed in environmentally controlled and specific conditions. After adaptive feeding for a week, the rats were divided into 3 groups, including the control group, SS group, and ST group, with 5 rats in each group. SS and ST were intragastrically administered to the corresponding group at 2 g/kg at a time.[33–35] Rats in the control group were intragastrically administered an equal vehicle volume of CMC-Na solution at a time. The mental status, food intake, and body weight of the rats were observed and recorded for 14.[36,37] At the end of the experiment, the weights of the liver, spleen, and kidney were recorded. The animal protocol of this study was approved by the Animal Ethics Committee of Nanjing University of Traditional Chinese Medicine (approval no. 202112A022). All the animals received humane care according to the guidelines of the National Institutes of Health (USA).

Induction of Liver Toxicity

Male C57BL/6J mice (6–8 weeks, 20~22 g) were purchased from Weitonglihua (Nanjing, China) and housed in environmentally controlled and specific conditions. After adaptive feeding for a week, the mice were divided into 7 groups, including the control group (C), model group (M), Sil group (0.2 mmol/kg) (Sil), 1/2 SS group (0.1 mmol/kg) (1/2 SS), SS group (0.2 mmol/kg) (SS), 1/2 ST group (0.1 mmol/kg) (1/2 ST), and ST group (0.2 mmol/kg) (ST), with 8 mice in each group. Mice were intragastrically administered the corresponding drugs once a day for 7 d continuously. Mice in the control

and model groups were given drug-free CMC-Na solution. On Day 7, all mice were injected intraperitoneally with 0.5% CCl_4 (dissolved in olive oil, 0.1 mL/10 g body weight) 1 h after the last dose, except for the control group, which was injected intraperitoneally with olive oil. Mice were anesthetized with 1.5% isoflurane after 24 h of fasting, and blood was collected via the retro-orbital sinus plexus. All mice were then sacrificed, and their livers were dissected and used for histopathological (formalin-fixed) and biochemical (−80 °C) studies.[24,38,39] The animal protocol of this study was approved by the Animal Ethics Committee of Nanjing University of Traditional Chinese Medicine (approval no. 202112A021). All the animals received humane care according to the guidelines of the National Institutes of Health.

Hematology and Serum Biochemistry

The blood used for routine blood analysis was stored in EDTA-K2 anticoagulation tubes, and various indicators, such as red blood cell count (RBC), hemoglobin (HGB), and white blood cells (WBCs), were analyzed. Blood samples for serum biochemical analysis were placed in plain tubes without anticoagulants and left at room temperature for 15–20 min. After the blood had clotted, the serum was collected by centrifugation at 3000× g for 15 min at 4 °C. The serum was analyzed for biochemical indices, such as glutamate aminotransferase (ALT), aspartate aminotransferase (AST), urea, and creatinine.

Histopathology

Liver tissues were fixed in 4% paraformaldehyde (Servicebio, # G1101-500ML, Wuhan). Liver tissue was dehydrated in an embedding kit (75% ethanol for 6 hours, 85% ethanol for 10 hours, 95% ethanol for 4 hours, ethanol I for 2 hours, ethanol II for 2 hours), cleared (xylene I for 20 minutes, xylene II for 15 minutes), paraffin-impregnated for 3 hours, and finally embedded. The samples were cut into 5 μm slices, flattened on slides, and then incubated at 60 °C for more than 60 min. After multiple dewaxing steps in xylene, the sections were rinsed with water for 20 minutes, stained with hematoxylin (Biosharp, # BL700A, Hefei) for 30 seconds, rinsed again with water, and placed in 1% hydrochloric acid ethanol for several seconds. The sections were sequentially dehydrated in 70%, 85%, and 95% ethanol and then stained with eosin (Biosharp, # BL700A, Hefei) for 30 seconds. The sections were placed in anhydrous ethanol and xylene for 5 minutes sequentially. Finally, the slices were sealed with neutral resin glue, and images were acquired under a microscope (Olympus IX71, Japan).

To assess the degree of necrosis after acute liver injury, an injury grading scale (grades 0–4) was performed according to the severity of necrotic lesions in the liver parenchyma. The scoring system was as follows: grade 0, no pathological changes; grade 1, hepatocellular degeneration with only rare foci of necrosis; grade 2, small areas of mild central lobular necrosis around the central vein; grade 3, areas of mild central lobular necrosis more severe than grade 2; and grade 4, central lobular necrosis more severe than grade 3.[24]

Immunohistochemical Analysis (IHC)

Liver tissue was fixed in 4% paraformaldehyde (Servicebio, # G1101-500ML, Wuhan), embedded in paraffin wax and cut into 4 μm sections. Then, the sections were hydrated to remove the paraffin. Endogenous peroxidase activity was then blocked with hydrogen peroxide for 15 mins. Antigen repair was performed by boiling in 10 mM citrate buffer for 10 mins, and then the sections were incubated with the primary antibody (F4/80 (D2S9R) (dilution 1:600)) and placed in the refrigerator at 4 °C overnight. The sections were incubated for 1 h at room temperature with the addition of the corresponding secondary antibody. Finally, the specimens were stained with the DAB kit. The samples were washed with PBS, and images were acquired under a microscope (Olympus IX71, Japan).

TdT-Mediated dUTP Nick End Labeling (TUNEL)

Apoptosis in liver tissue was detected using the Terminal Deoxynucleotidyl Transferase-Mediated dUTP Notched End Labeling (TUNEL) assay kit (KeyGEN BioTECH, #KGA7061, Nanjing). After TUNEL labeling, liver sections were restained with an anti-fluorescence attenuation quencher containing DAPI (Solarbio, #S2110, Beijing) to label nuclei. Images were observed under a fluorescence microscope (Olympus IX71, Japan).

Western Blotting (WB)

Liver tissues were collected from mice and disrupted in RIPA (Beyotime Biotechnology, #P0013B, Shanghai) mixed with PMSF (Keygenbio, #KGP610, Nanjing) on ice. Proteins (100 μg) were separated by 10% sodium dodecyl sulfate–polyacrylamide gel electrophoresis (SDS–PAGE) (BIO-RAD, #1705061, California) and then transferred to a PVDF membrane (BIO-RAD, #1620256, California). The membranes were blocked in Tris-buffered saline Tween-20 (TBST) containing 5% skim milk (BioFroxx, # 3250GR500, Germany) for 1 h at room temperature, followed by incubation with primary antibodies against p53 (1:1000, Cell Signaling Technology, #2527, Boston), PARP (1:1000, Cell Signaling Technology, #9523, Boston), BCl-2 (1:1000, Abcam, #ab32124, Cambridge), Bax (1:2000, Abcam, #ab182733, Cambridge), and β-actin (1:1000, Cell Signaling Technology, #3700, Boston) at 4 °C overnight. The membranes were washed three times with TBST and then incubated with HRP-conjugated anti-rabbit IgG (1:2000, Cell Signaling Technology, #7074, Boston) and HRP-conjugated anti-mouse IgG (1:2000, Cell Signaling Technology, #7076, Boston) for 1 h at room temperature. After washing with TBST three times, the antibodies were detected with ECL reagents (Tanon, #180-506, Shanghai). Immunoreactivity was detected by chemiluminescence. The results were quantified using ImageJ software.

Quantitative Real-Time Polymerase Chain Reaction (qRT–PCR) Analysis

Total RNA was extracted from liver tissues using TRIzol reagent (Thermo Fisher, #15596026, Waltham). Equal amounts of RNA (5000 ng) were reverse transcribed into cDNA using an All-in-One First-Strand cDNA Synthesis SuperMix for qPCR (One-Step gDNA Removal) (TransGen Biotech, #AE341, Beijing) according to the manufacturer's protocols on a Real-Time PCR System (Applied Biosystems, #9902, Waltham). Quantitative real-time PCR (QPCR) was performed using Top Green qPCR SuperMix (TransGen Biotech, #AQ132, Beijing) on a Real-Time PCR System (Applied Biosystems, #Q6, Waltham). Details of the primers can be found in Table 2. The relative quantification of real-time RT–PCR products was performed using the $2^{-\Delta\Delta CT}$ method.

Molecular Docking

Docking experiments were performed and completed by the Molecular Operating Environment (MOE). The crystal structures of the proteins were obtained from the Protein Data Bank (PDB). Preparation of compound structures, protein structures (proton 3-D and energy minimization), determination of active sites, and docking procedures were performed according to previously described procedures.[40,41]

Statistical Analysis

All data were obtained from at least three parallel sets of experiments and are expressed as the means ± SD. Statistical analyses were performed using GraphPad Prism V.8.00. Between-group analyses were performed using one-way ANOVA followed by Tukey post hoc analysis, and p values <0.05 were considered statistically significant.

All data are expressed as the means ± standard errors of means. The data obtained from cultured cells and animals were analyzed using Student's *t*-test and one-way ANOVA to determine the significance of the difference between two groups and are presented as the means ± SD from independent experiments via GraphPad Prism 8. P<0.05 was considered statistically significant.

Table 2 Primers Used for qRT–PCR Analysis

Gene Name	Forward Primer Sequence (5'-3')	Reverse Primer Sequence (5'-3')
IL-1β	GAAATGCCACCTTTTGACAGTG	TGGATGCTCTCATCAGGACAG
IL-6	TAGTCCTTCCTACCCCAATTTCC	TTGGTCCTTAGCCACTCCTTC
TNF-α	GGGGATACATCCATCAGGGGT	GCTCGGACAGTCACTCACC
IL-10	CTTACTGACTGGCATGAGGATCA	GCAGCTCTAGGAGCATGTGG
GAPDH	CAGTATGACTCCACTCACGGCAA	CTCGCTCCTGGAAGATGGTGAT

Results

SS and ST Significantly Improve the in vitro Solubility of Sil

The corresponding derivatives were obtained by the dehydration condensation of the carbonyl group in Sil and the amino group in amino acids through the Schiff base reaction. SS and ST are two derivatives obtained from S-allyl-L-cysteine and taurine as ligands, respectively. The solubility of SS and ST in pure water was greater than 125 mg/mL, and the water solubility was significantly improved compared to that of Sil.

During purification using recrystallization of these two compounds, we found that large crystal particles could not form. Therefore, PLM and PXRD experimental analyses were performed, and the results showed that the physical forms of both compounds exhibited amorphous substances (Figure 2A and B). In the crystallographic screening experiments, no crystallographic transformation occurred in either SS or ST, which indicates that the amorphous properties of SS and ST are relatively stable.

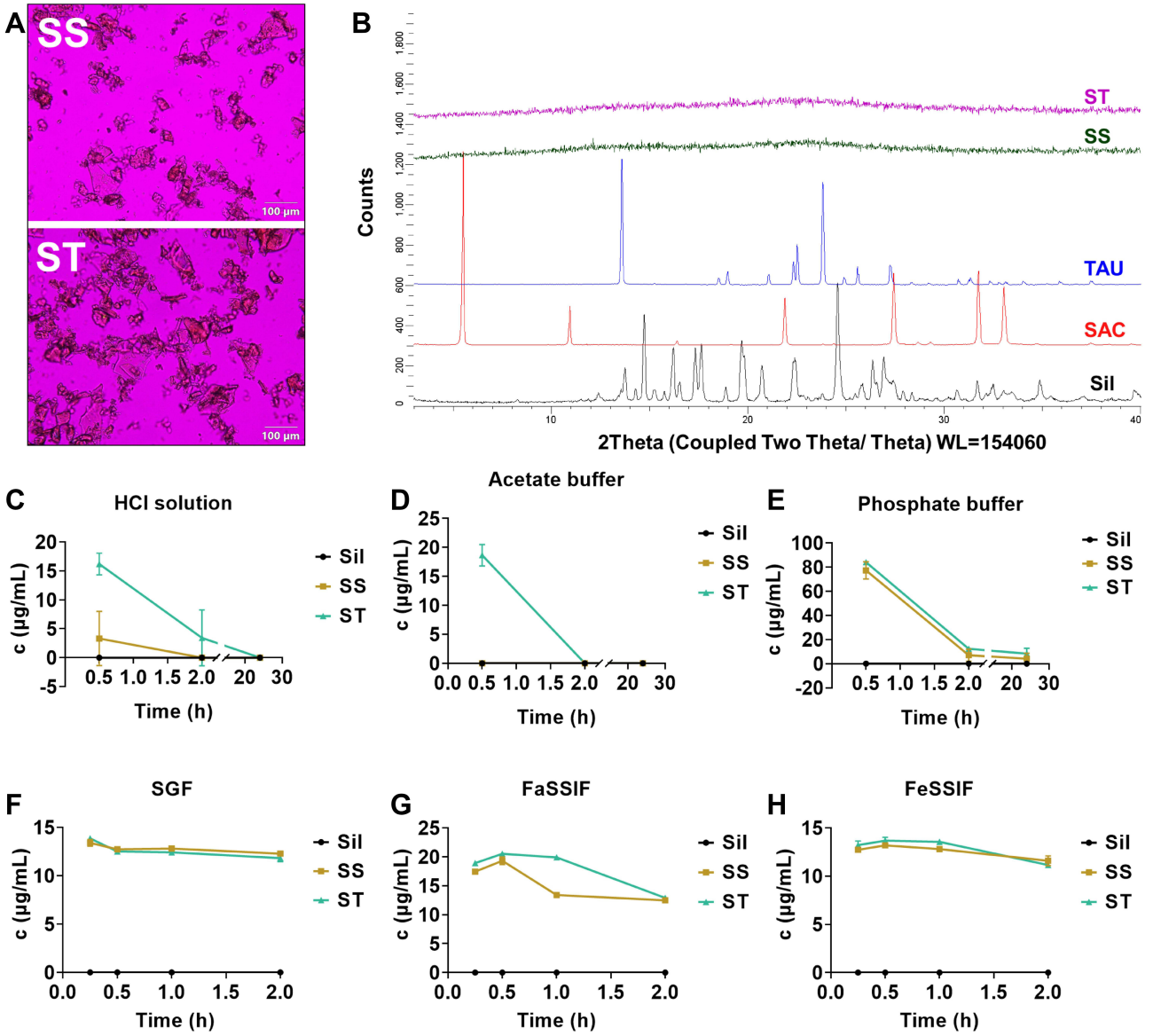

Figure 2 SS and ST observation under PLM (**A**). X-ray powder diffractograms of Sil, SAC, TAU, SS, and ST (**B**). Dynamic solubility of the Sil parent nucleus of SS and ST in six solutions (n=3) (**C**–**H**).

Due to the hydrophilic property of the ligand and the high solubility properties of the amorphous substance, in vitro solubility experiments were performed to simulate the dissolution of the drug in the stomach and intestine. The results showed that the pH of all six standard buffer solutions did not change significantly before and after the solubility experiment (Table S1), and the solubility of Sil in all six solutions fell below the instrument detection limit and was recorded as 0. SS and ST dissociated to varying degrees in six acidic media: HCl solution, acetate buffer, phosphate buffer, SGF, FaSSIF-v1, and FeSSIF-v1. SS and ST dissociated completely in the first three solutions after 2 h (Figure 2C–E), and they were maintained at 10~20 μg/mL (Figure 2F–H) in the latter three solutions. PXRD experimental analysis of the precipitate in the solution after 24 hours of revealed that the dissociated fraction was the parent nucleus of Sil (Figure S3). Therefore, we conjecture that SS and ST have better absorption than Sil and are able to isolate Sil after entering the organism. SS and ST might therefore be studied and applied as predrugs of Sil.

SS and ST Show Good Safety Profiles in vitro and in vivo

To evaluate the biosafety of both compounds (SS and ST), separate studies were performed on cells (in vitro) and animals (in vivo). First, LO-2 cells were stimulated by selecting different concentrations of compounds, and changes in cell viability were measured by both CCK-8 and LDH assays. The results showed that the cell viability was only slightly impaired at the high concentration of 48 μM in the CCK-8 assay (Figure 3A and B), but this concentration did not show a toxic response in the LDH assay (Figure 3C and D). The results showed that neither SS nor ST produced significant cytotoxic effects on cells at concentrations less than 24 μM.

Subsequently, we assessed the safety of the compounds by acute toxicity assays in rats, observing and recording the physiological responses of the animals for 2 weeks after administration (Figure 3E). The rats in each group either did not show an abnormal status or died during the experiment. The data showed no significant differences in body weight gain (Figure 3F), daily food intake (Figure 3G), or weekly food utilization (Figure 3H) among the three groups of rats during the two-week observation period. This indicates that SS and ST did not adversely affect the growth of rats. In addition, there were no significant differences in the ratios of each organ (liver, spleen, and kidney) to body weight in the three groups of rats (Figure 3I). The results of routine blood examination in rats (Figure 3J–L) showed no significant differences, except for the leukocyte count index in the SS group, which was slightly lower than that in the C group (Figure 3L). In addition, no damage or lesions were observed when the livers of the rats in each group were examined pathologically (Figure 3M). Overall, no significant mortality or physiological abnormalities were observed in the animals at such extreme doses, and the biosafety of SS and ST was positive.

SS and ST Reduce CCl_4-Induced Hepatocyte Necrosis More Than Sil

To evaluate whether the hepatoprotective activity of SS and ST was improved compared with that of Sil, CCl_4-induced acute liver injury was selected as an animal model for bioactivity evaluation in this study (Figure 4A).

First, histopathological examination by H&E staining showed obvious necrotic areas in Group M, with disappearance of cell borders and destruction of liver structure (Figure 4B), and the pathology of the liver tissue was scored in each group (Figure 4C). Pretreatment with Sil, SS, or ST reduced liver injury morphologically compared to the M group; furthermore, SS and ST exhibited milder hepatocyte necrosis and better preservation of liver structure at equimolar doses administered with Sil. The effects of SS and ST pretreatment on CCl_4-induced acute liver injury were then evaluated by measuring the release of two serum aminotransferases (glutamate aminotransferase (ALT) and aspartate aminotransferase (AST)). The results showed that the serum aminotransferase levels of rats in the M group were significantly higher than those in the C group, and SS and ST significantly reduced the CCl_4-induced increase in transaminase levels compared to Sil. Moreover, the SS and ST release levels were close to those of the C group compared with the equimolar Sil group (Figure 4D and E).

In combination with serum transaminase release levels and histopathological observations, SS and ST exhibited greater resistance to CCl_4-induced acute liver injury than Sil when administered at equimolar doses.

SS and ST Better Reduce CCl_4-Induced Liver Inflammation Than Sil

The elevated inflammatory response of CCl_4 is an important indicator of acute liver injury and is part of the pathogenesis of most liver precursor diseases. The expression of proinflammatory factors (TNF-α, IL-6, and IL-1β) in the SS and ST groups was significantly lower than that in the Sil group (Figure 5A–C), and the expression of an anti-inflammatory

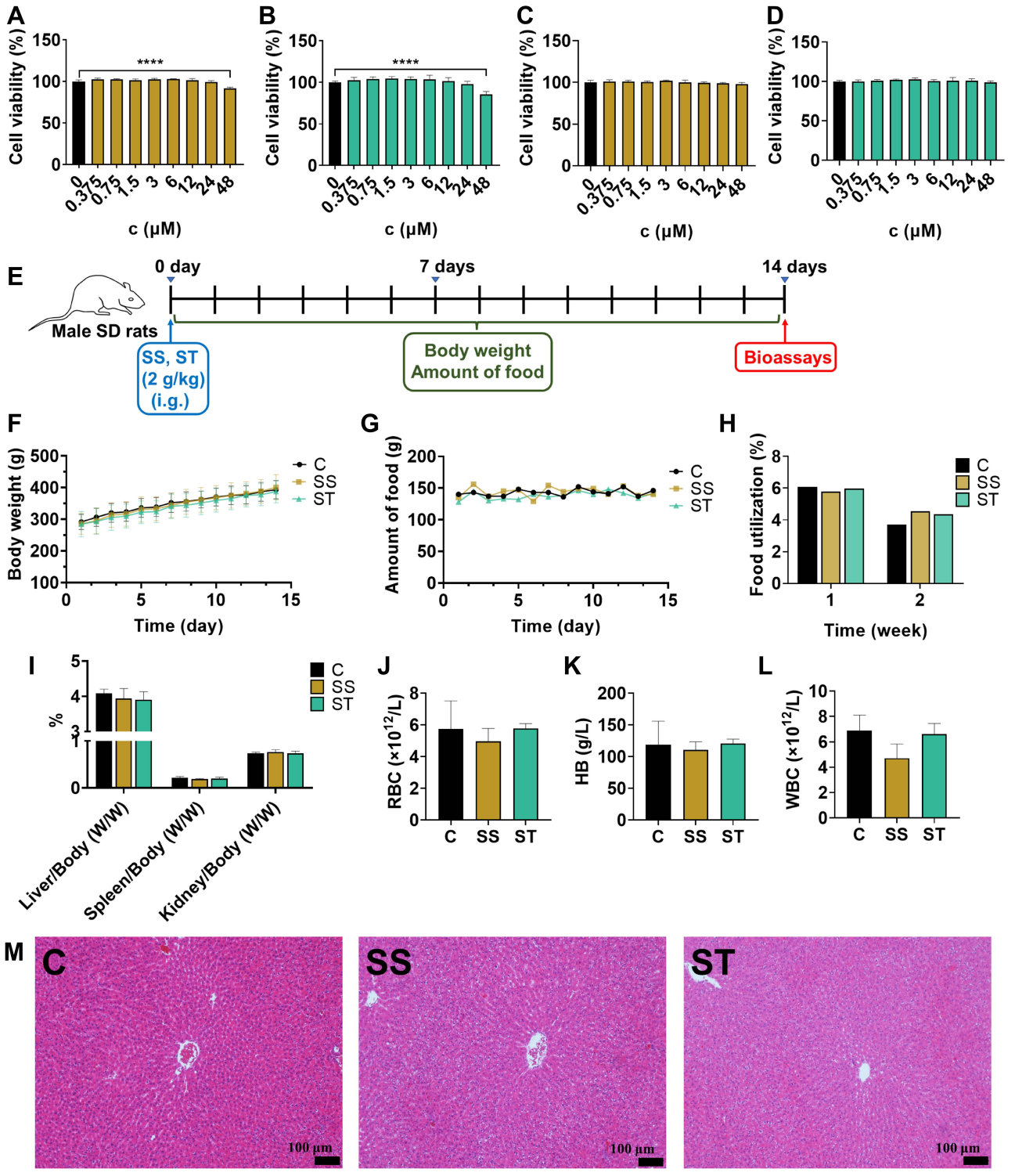

Figure 3 Cytotoxicity of SS (**A**) and ST (**B**) against LO-2 cells as detected by CCK-8 assay (n=6). Cytotoxicity of SS (**C**) and ST (**D**) against LO-2 cells as detected by LDH assay (n=6). Experimental protocol for acute toxicity in rats (**E**). Daily body weight (**F**), daily food intake (**G**), and weekly food utilization of rats (**H**) after administration (n=5). Liver/body weight, kidney/body weight, and spleen/body weight of rats after the experiment (n=5) (**I**). The results of routine blood tests in rats at the end of the experiment (n=3~5) (**J**–**L**). Histopathological observation of the liver of SD rats after acute toxicity experiments (**M**). Hematoxylin-eosin staining of liver paraffin sections showing areas of liver damage (black arrows) (scale bar = 100 μm). ****p<0.0001.

factor (IL-10) in the SS and ST groups was the highest among all drug pretreatment groups (Figure 5D). The improvement of inflammatory factors in serum indicates that SS and ST reduced the inflammatory response induced by CCl_4 at the overall animal level.

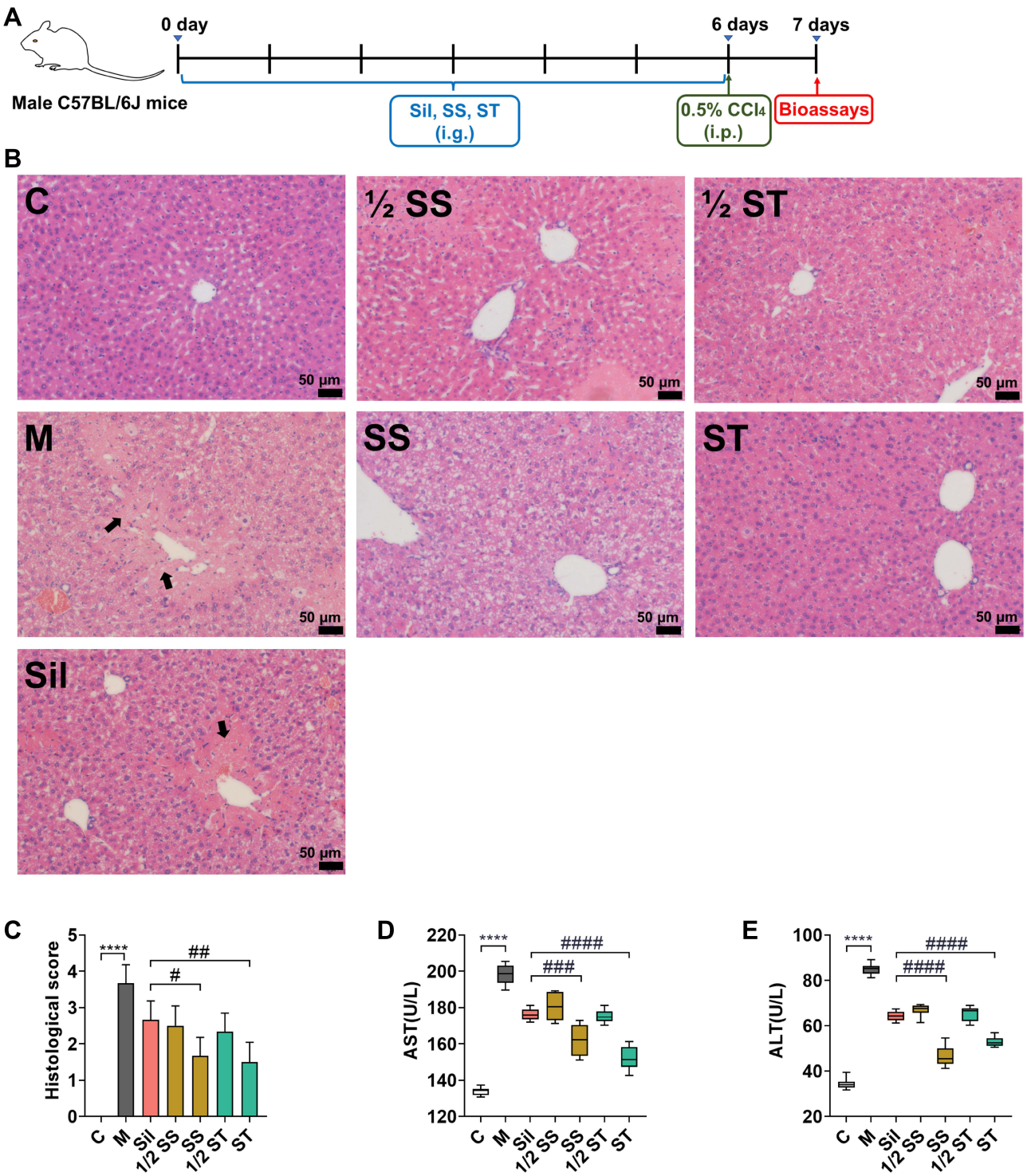

Figure 4 Experimental protocol of drugs used to treat CCl_4-induced acute liver injury (**A**). Effect of SS and ST on histopathology following CCl_4-induced liver injury in mice (**B**). Hematoxylin-eosin staining of paraffin sections of the liver, showing areas of liver injury (black arrows) (scale bar=50 μm). Liver sections from seven groups of mice were scored histologically (n=5) (**C**). Effect of SS and ST on the levels of AST (n=8) (**D**) and ALT (n=8) (**E**) release in the serum of CCl_4-treated mice. ****p<0.0001, $^{\#}$p<0.05, $^{\#\#}$p<0.01, $^{\#\#\#}$p<0.001, $^{\#\#\#\#}$p<0.0001.

Additionally, liver tissue sections were stained with macrophage markers (F4/80) to observe the extent of macrophage infiltration and to assess the degree of the inflammatory response and effect of drug pretreatment. The results showed that all dosing groups significantly reduced macrophage infiltration, and the SS and ST groups were significantly more effective than the Sil group (Figure 5E and F). The expression of relevant inflammatory factor mRNAs in liver tissue was

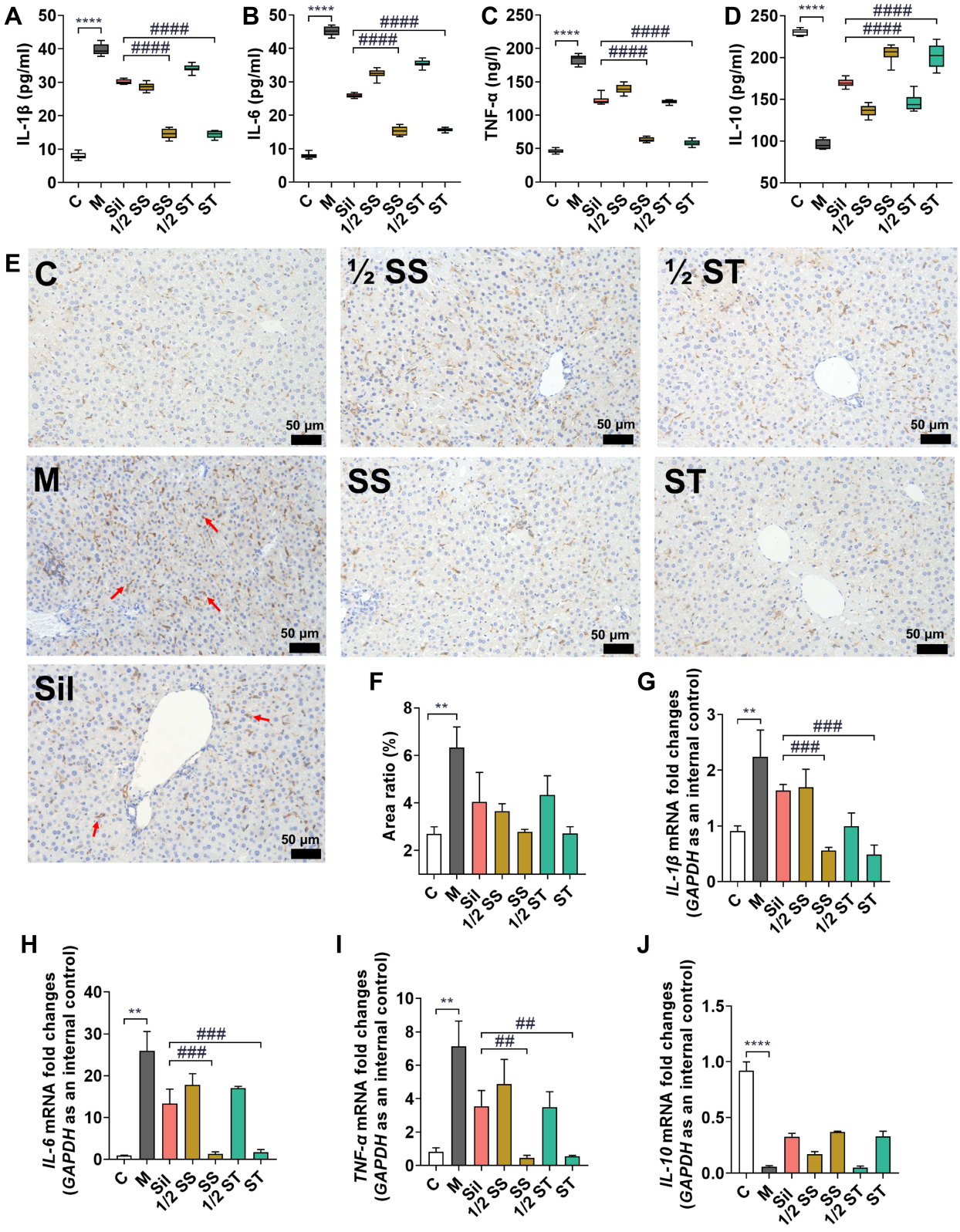

Figure 5 Expression levels of four inflammatory factors in serum (**A–D**). Macrophage staining of paraffin sections of liver (red arrows) (scale bar=50 μm) (**E**). Analysis of the area percentage of macrophage infiltration (**F**). The mRNA expression levels of four inflammatory factors in liver tissues (**G–J**). **p<0.01, ****p<0.0001, ##p<0.01, ###p<0.001, ####p<0.0001.

consistent with the results of serum biochemical indices, further suggesting that SS and ST could better ameliorate the inflammatory response induced by CCl_4 than Sil (Figure 5G–J).

SS and ST are More Efficient Than Sil at Attenuating CCl_4-Induced Apoptosis

Hepatocyte apoptosis is an important feature of CCl_4-induced liver injury; as a cellular response to hepatotoxic injury, it can reflect the extent of liver injury. The results of the TdT-mediated dUTP nick-end labeling (TUNEL) assay showed that CCl_4 caused extensive apoptosis in periportal hepatocytes, and it is noteworthy that SS and ST pretreatment significantly reduced the number of TUNEL-positive apoptotic hepatocytes compared with the same dose of Sil pretreatment (Figure 6A and B). Subsequently, Western blot experiments were performed to measure the expression levels of apoptosis-related proteins in the liver. The experimental results showed that CCl_4 significantly reduced the expression of PPAR, Bcl-2, and Bax. This phenomenon was reversed by pretreatment with SS, ST, and Sil, and the improvement was particularly evident in the SS and ST groups (Figure 6C–G). Notably, CCl_4 increased the expression of p53 in the liver, and pretreatment further increased the expression of this protein (Figure 6C–E). Thus, CCl_4-induced elevation of p53 protein may be a feedback protective mechanism to induce apoptosis after severe

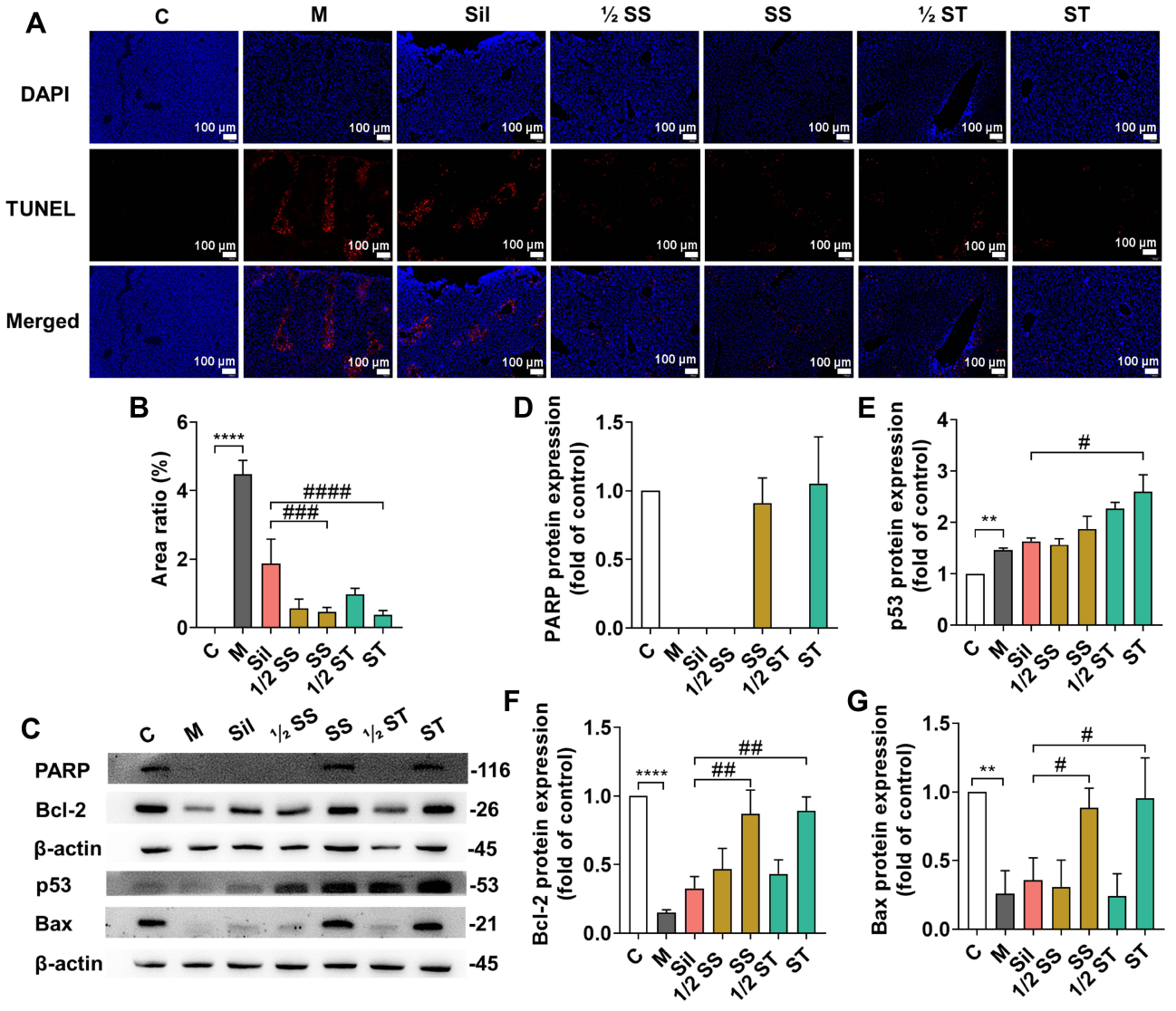

Figure 6 Apoptosis was detected by the TUNEL method (scale bar=100 μm) (**A**). Analysis of the apoptotic area according to the TUNEL staining assay (**B**). Western blotting was performed to detect the protein expression levels of PARP, p53, Bcl-2 and Bax in liver tissues (**C**–**G**). **p<0.01, ****p<0.0001, #p<0.05, ##p<0.01, ###p<0.001, ####p<0.0001.

liver injury and inhibit CCl_4-induced cell carcinogenesis. The specific hepatoprotective mechanism of Sil needs to be explored further, but these phenotypic results suggest that the anti-apoptotic effect of SS and ST is significantly superior to that of Sil.

Discussion

The liver plays a pivotal role in many physiological processes, including nutrient metabolism, immune system support, endocrine control, cholesterol homeostasis, and the breakdown of exogenous compounds.[42,43] A wide variety of liver diseases brought about by dietary habits and drug use have seriously affected people's health.[44,45] For a long time, silibinin has been used as a hepatoprotective drug in the clinical treatment of liver diseases and is by far the most widely studied and used natural hepatoprotective compound.[5,46,47] However, due to its structural limitations, the bioavailability of silibinin is not ideal,[48] and a slow onset of action often occurs during clinical use.

To overcome this drawback, previous studies have developed semisynthetic derivatives in terms of chemical structure modification. However, the one-sided grafting of hydrophilic groups makes the molecular weight of the derivatives too large, which may affect the interaction between silibinin and the target protein. Thus, the synthesis of a class of prodrugs that can dissociate the parent nucleus of silibinin under certain conditions can circumvent the previous problems of semisynthetic derivatives.[49–51]

In the present study, the derivatives obtained using the Schiff base reaction relied on hydrophilic and amorphous morphology to successfully improve the solubility of silibinin in biological media and were able to decompose the silibinin parent nucleus over time.

The biosafety of silibinin itself has been well established in previous studies and applications. However, the physical properties of SS and ST, as semisynthetic derivatives of silibinin, have been changed to some extent. It is necessary to discuss and study the biosafety of these two derivatives to guide the selection of "safe" doses in subsequent studies.[36,37] The results of the toxicity experiments in this study showed that SS and ST exhibited good low toxicity against both LO-2 cells and SD rats.

A model of acute liver injury due to CCl_4 is often chosen for the screening and activity evaluation of hepatoprotective drugs. This model exhibits a strong inflammatory response and high levels of apoptosis.[52–55] This is consistent with the results of the present study. It is important to emphasize that SS and ST at equimolar doses administered with silibinin more significantly reduced the expression of proinflammatory factors in the liver and also better regulated the expression of apoptosis-related proteins.

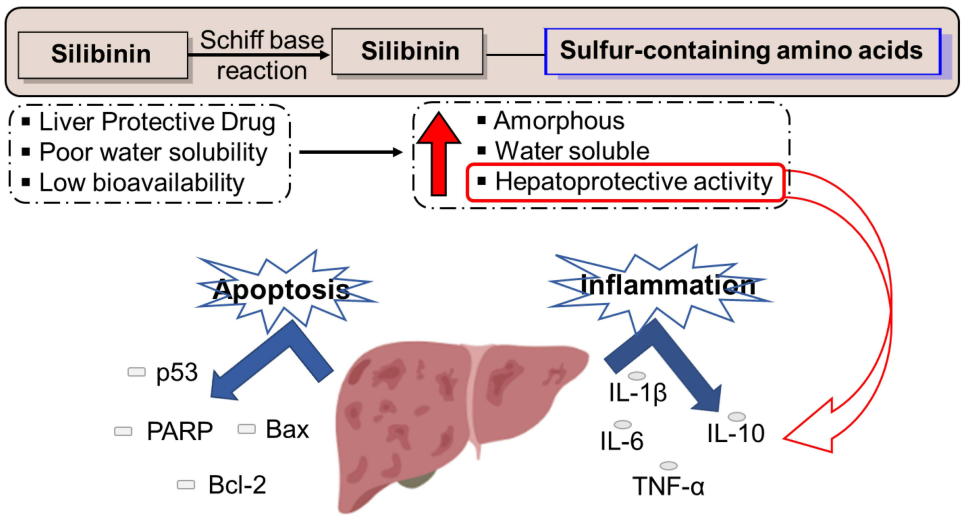

Figure 7 Silibinin Schiff base derivatives (SS and ST) enhance both the anti-inflammatory and anti-apoptotic activities of silibinin.

Conclusion

In summary, two new water-soluble silibinin Schiff base derivatives were developed in this study. The safety of both derivatives was demonstrated by in vitro in vivo toxicity experiments. The biological activities (anti-inflammatory and anti-apoptotic) of both derivatives were superior to silibinin in CCl_4-induced acute liver injury experiments (Figure 7). In conclusion, SS and ST are expected to be safe and effective alternatives to silibinin.

Abbreviations

Sil, silibinin; PXRD, powder X-ray diffraction; PLM, polarized light microscope; RBC, red blood cell count; HGB, hemoglobin; WBC, white blood cells; ALT, glutamate aminotransferase; AST, aspartate aminotransferase; IL-1β, interleukin-1β; IL-6, interleukin-6; TNF-α, tumor necrosis factor-α; IL-10, interleukin-10; GAPDH, glyceraldehyde-3-phosphate dehydrogenase; IHC, immunohistochemical; TUNEL, TdT-mediated dUTP nick end labeling; WB, Western blotting; qRT-PCR, quantitative real-time polymerase chain reaction analysis; SGF, simulated gastric fluid; FaSSIF, fasted state simulated intestinal fluid; FeSSIF, fed state simulated intestinal fluid.

Acknowledgments

This study was supported by Key Project of Jiangsu Province for Fundamental Research and Development (BE2018717), Specially-appointed Professor Grant by Jiangsu province (2014, Prof. Jing Zhu), Jiangsu Six Talent Peak Award (2015, Prof. Jing Zhu). We thank Prof. Jing Zhu and Ms. Xiaoli Liu for their careful guidance. Rong Xu and Siyan Qiu are co-first authors for this study.

Author Contributions

All authors made a significant contribution to the work reported, whether that is in the conception, study design, execution, acquisition of data, analysis and interpretation, or in all these areas; took part in drafting, revising or critically reviewing the article; gave final approval of the version to be published; have agreed on the journal to which the article has been submitted; and agree to be accountable for all aspects of the work.

Funding

This study was supported by Key Project of Jiangsu Province for Fundamental Research and Development (BE2018717), Specially-appointed Professor Grant by Jiangsu province (2014, Prof. Jing Zhu), Jiangsu Six Talent Peak Award (2015, Prof. Jing Zhu).

Disclosure

The authors report no conflicts of interest in this work.

References

1. Bijak M. Silybin, a major bioactive component of milk thistle (Silybum marianum L. Gaernt.)-chemistry, bioavailability, and metabolism. *Molecules*. 2017;22:1942.
2. Loguercio C, Festi D. Silybin and the liver: from basic research to clinical practice. *World J Gastroenterol*. 2011;17:2288–2301. doi:10.3748/wjg.v17.i18.2288
3. Federico A, Dallio M, Loguercio C. Silymarin/Silybin and chronic liver disease: a marriage of many years. *Molecules*. 2017;22:191. doi:10.3390/molecules22020191
4. Tajmohammadi A, Razavi BM, Hosseinzadeh H. Silybum marianum (milk thistle) and its main constituent, silymarin, as a potential therapeutic plant in metabolic syndrome: a review. *Phytother Res*. 2018;32:1933–1949. doi:10.1002/ptr.6153
5. Abenavoli L, Izzo AA, Milic N, Cicala C, Santini A, Capasso R. Milk thistle (Silybum marianum): a concise overview on its chemistry, pharmacological, and nutraceutical uses in liver diseases. *Phytother Res*. 2018;32:2202–2213. doi:10.1002/ptr.6171
6. Di Costanzo A, Angelico R. Formulation strategies for enhancing the bioavailability of silymarin: the state of the art. *Molecules*. 2019;24:2155. doi:10.3390/molecules24112155
7. Wu JW, Lin LC, Hung SC, Chi CW, Tsai TH. Analysis of silibinin in rat plasma and bile for hepatobiliary excretion and oral bioavailability application. *J Pharm Biomed Anal*. 2007;45:635–641. doi:10.1016/j.jpba.2007.06.026
8. Biedermann D, Vavrikova E, Cvak L, Kren V. Chemistry of silybin. *Nat Prod Rep*. 2014;31:1138–1157. doi:10.1039/C3NP70122K

9. Sala F, Albares P, Colovic M, Persiani S, Rovati LC. Development and validation of two liquid chromatography-tandem mass spectrometry methods for the determination of silibinin and silibinin hemisuccinate in human plasma. *J Chromatogr B Analyt Technol Biomed Life Sci*. 2014;945–946:1–9. doi:10.1016/j.jchromb.2013.11.028
10. Schramm S, Gunesch S, Lang F, et al. Investigations into neuroprotectivity, stability, and water solubility of 7-O-cinnamoylsilibinin, its hemisuccinate and dehydro derivatives. *Arch Pharm*. 2018;351:e1800206. doi:10.1002/ardp.201800206
11. Cufi S, Bonavia R, Vazquez-Martin A, et al. Silibinin meglumine, a water-soluble form of milk thistle silymarin, is an orally active anti-cancer agent that impedes the epithelial-to-mesenchymal transition (EMT) in EGFR-mutant non-small-cell lung carcinoma cells. *Food Chem Toxicol*. 2013;60:360–368. doi:10.1016/j.fct.2013.07.063
12. Chi C, Zhang C, Liu Y, Nie H, Zhou J, Ding Y. Phytosome-nanosuspensions for silybin-phospholipid complex with increased bioavailability and hepatoprotection efficacy. *Eur J Pharm Sci*. 2020;144:105212. doi:10.1016/j.ejps.2020.105212
13. He J, Chen Z, Gu Y, et al. Hydrophilic co-assemblies of two hydrophobic biomolecules improving the bioavailability of silybin. *Food Funct*. 2020;11:10828–10838. doi:10.1039/D0FO01882A
14. Zhang H, Wang CB, Liu JL. Silybin nanoparticles for liver cancer: development, optimization and in vitro - in vivo evaluation. *J BUON*. 2016;21:633–644.
15. Luo Y, Gong C, Wei M, et al. Evaluation of mogroside V as a promising carrier in drug delivery: improving the bioavailability and liver distribution of silybin. *AAPS PharmSciTech*. 2020;21:123. doi:10.1208/s12249-020-01645-9
16. Lu C, Li X, Liang X, et al. Liver targeting albumin-coated silybin-phospholipid particles prepared by nab technology for improving treatment effect of acute liver damage in intravenous administration. *AAPS PharmSciTech*. 2019;20:293. doi:10.1208/s12249-019-1504-y
17. Yi T, Liu C, Zhang J, Wang F, Wang J, Zhang J. A new drug nanocrystal self-stabilized Pickering emulsion for oral delivery of silybin. *Eur J Pharm Sci*. 2017;96:420–427. doi:10.1016/j.ejps.2016.08.047
18. Eriksson S, Prigge JR, Talago EA, Arner ES, Schmidt EE. Dietary methionine can sustain cytosolic redox homeostasis in the mouse liver. *Nat Commun*. 2015;6:6479. doi:10.1038/ncomms7479
19. Francioso A, Baseggio Conrado A, Mosca L, Fontana M. Chemistry and biochemistry of sulfur natural compounds: key intermediates of metabolism and redox biology. *Oxid Med Cell Longev*. 2020;2020:8294158. doi:10.1155/2020/8294158
20. Sies H, Reichert AS. Selectively addressing mitochondrial glutathione and thioredoxin redox systems. *Cell Chem Biol*. 2019;26:316–318. doi:10.1016/j.chembiol.2019.02.017
21. Zhao C, Rakesh KP, Ravidar L, Fang WY, Qin HL. Pharmaceutical and medicinal significance of sulfur (S(VI))-containing motifs for drug discovery: a critical review. *Eur J Med Chem*. 2019;162:679–734. doi:10.1016/j.ejmech.2018.11.017
22. Lau N, Pluth MD. Reactive sulfur species (RSS): persulfides, polysulfides, potential, and problems. *Curr Opin Chem Biol*. 2019;49:1–8. doi:10.1016/j.cbpa.2018.08.012
23. Li S, Liu J, Zhang M, Chen Y, Zhu T, Wang J. Protective effect of eckol against acute hepatic injury induced by carbon tetrachloride in mice. *Mar Drugs*. 2018;16:300. doi:10.3390/md16090300
24. Dai C, Xiao X, Li D, et al. Chloroquine ameliorates carbon tetrachloride-induced acute liver injury in mice via the concomitant inhibition of inflammation and induction of apoptosis. *Cell Death Dis*. 2018;9:1164. doi:10.1038/s41419-018-1136-2
25. Meng X, Tang GY, Liu PH, Zhao CJ, Liu Q, Li HB. Antioxidant activity and hepatoprotective effect of 10 medicinal herbs on CCl4-induced liver injury in mice. *World J Gastroenterol*. 2020;26:5629–5645. doi:10.3748/wjg.v26.i37.5629
26. Ratha P, Chitra L, Ancy I, Kumaradhas P, Palvannan T. New amino acid-Schiff base derived from s-allyl cysteine and methionine alleviates carbon tetrachloride-induced liver dysfunction. *Biochimie*. 2017;138:70–81. doi:10.1016/j.biochi.2017.04.010
27. Taleb A, Ahmad KA, Ihsan AU, et al. Antioxidant effects and mechanism of silymarin in oxidative stress induced cardiovascular diseases. *Biomed Pharmacother*. 2018;102:689–698. doi:10.1016/j.biopha.2018.03.140
28. Ferraz AC, Almeida LT, da Silva Caetano CC, et al. Hepatoprotective, antioxidant, anti-inflammatory, and antiviral activities of silymarin against Mayaro virus infection. *Antiviral Res*. 2021;194:105168. doi:10.1016/j.antiviral.2021.105168
29. Chen SM, Zou Z, Guo SY, et al. Preventing Candida albicans from subverting host plasminogen for invasive infection treatment. *Emerg Microbes Infect*. 2020;9:2417–2432. doi:10.1080/22221751.2020.1840927
30. Sun Q, Kang RR, Chen KG, et al. Sirtuin 3 is required for the protective effect of resveratrol on manganese-induced disruption of mitochondrial biogenesis in primary cultured neurons. *J Neurochem*. 2021;156:121–135. doi:10.1111/jnc.15095
31. Tian K, Wang A, Wang J, et al. Transcriptome analysis identifies SenZfp536, a sense LncRNA that suppresses self-renewal of cortical neural progenitors. *Neurosci Bull*. 2021;37:183–200. doi:10.1007/s12264-020-00607-2
32. Lu X, Gan Q, Gan C, et al. Long non-coding RNA PICSAR knockdown inhibits the progression of cutaneous squamous cell carcinoma by regulating miR-125b/YAP1 axis. *Life Sci*. 2021;274:118303. doi:10.1016/j.lfs.2020.118303
33. Upadhyay P, Shukla R, Mishra SK. Acute and sub-acute toxicity study of hydro-alcoholic leaves extract of Reinwardtia indica in rats. *Biomed Pharmacother*. 2019;111:36–41. doi:10.1016/j.biopha.2018.12.056
34. Al-Afifi NA, Alabsi AM, Bakri MM, Ramanathan A. Acute and sub-acute oral toxicity of Dracaena cinnabari resin methanol extract in rats. *BMC Complement Altern Med*. 2018;18:50. doi:10.1186/s12906-018-2110-3
35. Deyno S, Abebe A, Tola MA, et al. Acute and sub-acute toxicity of Echinops kebericho decoction in rats. *BMC Complement Med Ther*. 2020;20:2. doi:10.1186/s12906-019-2794-z
36. Prabu PC, Panchapakesan S, Raj CD. Acute and sub-acute oral toxicity assessment of the hydroalcoholic extract of Withania somnifera roots in Wistar rats. *Phytother Res*. 2013;27:1169–1178. doi:10.1002/ptr.4854
37. Li Y, Zhuang Y, Tian W, Sun L. In vivo acute and subacute toxicities of phenolic extract from rambutan (Nephelium lappaceum) peels by oral administration. *Food Chem*. 2020;320:126618. doi:10.1016/j.foodchem.2020.126618
38. Zhao ZW, Chang JC, Lin LW, Tsai FH, Chang HC, Wu CR. Comparison of the hepatoprotective effects of four endemic Cirsium species extracts from Taiwan on CCl(4)-induced acute liver damage in C57BL/6 mice. *Int J Mol Sci*. 2018;19:1329. doi:10.3390/ijms19051329
39. Xie J, Liu J, Chen TM, et al. Dihydromyricetin alleviates carbon tetrachloride-induced acute liver injury via JNK-dependent mechanism in mice. *World J Gastroenterol*. 2015;21:5473–5481. doi:10.3748/wjg.v21.i18.5473
40. Iftikhar F, Ali Y, Ahmad Kiani F, et al. Design, synthesis, in vitro evaluation and docking studies on dihydropyrimidine-based urease inhibitors. *Bioorg Chem*. 2017;74:53–65. doi:10.1016/j.bioorg.2017.07.003

41. Rashid U, Sultana R, Shaheen N, et al. Structure based medicinal chemistry-driven strategy to design substituted dihydropyrimidines as potential antileishmanial agents. *Eur J Med Chem*. 2016;115:230–244. doi:10.1016/j.ejmech.2016.03.022
42. Trefts E, Gannon M, Wasserman DH. The liver. *Curr Biol*. 2017;27:R1147–R1151. doi:10.1016/j.cub.2017.09.019
43. Gruppuso PA, Sanders JA. Regulation of liver development: implications for liver biology across the lifespan. *J Mol Endocrinol*. 2016;56:R115–R125. doi:10.1530/JME-15-0313
44. Lemmer P, Manka P, Best J, et al. Effects of moderate alcohol consumption in non-alcoholic fatty liver disease. *J Clin Med*. 2022;11:890. doi:10.3390/jcm11030890
45. Wang FS, Fan JG, Zhang Z, Gao B, Wang HY. The global burden of liver disease: the major impact of China. *Hepatology*. 2014;60:2099–2108. doi:10.1002/hep.27406
46. Abenavoli L, Capasso R, Milic N, Capasso F. Milk thistle in liver diseases: past, present, future. *Phytother Res*. 2010;24:1423–1432. doi:10.1002/ptr.3207
47. Polachi N, Bai G, Li T, et al. Modulatory effects of silibinin in various cell signaling pathways against liver disorders and cancer - A comprehensive review. *Eur J Med Chem*. 2016;123:577–595. doi:10.1016/j.ejmech.2016.07.070
48. Takke A, Shende P. Nanotherapeutic silibinin: an insight of phytomedicine in healthcare reformation. *Nanomedicine*. 2019;21:102057. doi:10.1016/j.nano.2019.102057
49. Zawilska JB, Wojcieszak J, Olejniczak AB. Prodrugs: a challenge for the drug development. *Pharmacol Rep*. 2013;65:1–14. doi:10.1016/S1734-1140(13)70959-9
50. Huttunen KM, Raunio H, Rautio J. Prodrugs–from serendipity to rational design. *Pharmacol Rev*. 2011;63:750–771. doi:10.1124/pr.110.003459
51. Walther R, Rautio J, Zelikin AN. Prodrugs in medicinal chemistry and enzyme prodrug therapies. *Adv Drug Deliv Rev*. 2017;118:65–77. doi:10.1016/j.addr.2017.06.013
52. Wang T, Zhou X, Kuang G, et al. Paeoniflorin modulates oxidative stress, inflammation and hepatic stellate cells activation to alleviate CCl4-induced hepatic fibrosis by upregulation of heme oxygenase-1 in mice. *J Pharm Pharmacol*. 2021;73:338–346. doi:10.1093/jpp/rgaa042
53. Peng Y, Huang K, Shen L, Tao YY, Liu CH. Cultured Mycelium Cordyceps sinensis allevi notates CCl4-induced liver inflammation and fibrosis in mice by activating hepatic natural killer cells. *Acta Pharmacol Sin*. 2016;37:204–216. doi:10.1038/aps.2015.129
54. Yang K, Zou Z, Wu Y, Hu G. MiR-195 suppression alleviates apoptosis and oxidative stress in CCl4-induced ALI in mice by targeting Pim-1. *Exp Mol Pathol*. 2020;115:104438. doi:10.1016/j.yexmp.2020.104438
55. Yang CL, Zheng XL, Ye K, et al. Effects of microRNA-217 on proliferation, apoptosis, and autophagy of hepatocytes in rat models of CCL4-induced liver injury by targeting NAT2. *J Cell Physiol*. 2019;234:3410–3424. doi:10.1002/jcp.26748